Metal-Containing Poly(ionic liquid) Exhibiting Photogeneration of Coordination Network: Reversible Control of Viscoelasticity and Ionic Conductivity

Sumitani, Ryo

Mochida, Tomoyuki

(Citation)
Macromolecules,53(16):6968-6974

(Issue Date)
2020-08-25

(Resource Type)
journal article

(Version)
Accepted Manuscript

Metal-Containing Poly(ionic liquid) Exhibiting Photogeneration of Coordination Network: Reversible Control of Viscoelasticity and Ionic Conductivity

Ryo Sumitani[a] *and Tomoyuki Mochida*[*a,b]

[a]Department of Chemistry, Graduate School of Science, Kobe University, Rokkodai, Nada, Kobe, Hyogo 657-8501, Japan. E-mail: tmochida@platinum.kobe-u.ac.jp

[b]Center for Membrane and Film Technology, Kobe University, Rokkodai, Nada, Kobe, Hyogo 657-8501, Japan.

TOC graphic

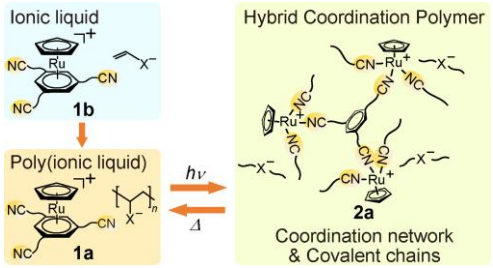

ABSTRACT: The control of physical properties of soft matters via external stimuli is useful for various applications. Poly(ionic liquid)s are versatile liquid polymers exhibiting ionic conductivity, though the development of photoresponsive poly(ionic liquid)s is still limited. Here we report the synthesis and properties of a photoreactive poly(ionic liquid) **1a** consisting

of a Ru sandwich complex $[Ru(C_5H_5)\{C_6H_3(OC_6H_{12}CN)_3\}]^+$ and a polymeric anion -[-CH_2-$CH(SO_2N^-SO_2CF_3)$-]$_n$-. Upon UV photoirradiation, the liquid transformed to a rubbery elastomer **2a** through the photochemical reaction of the cations. The resultant elastomer is a unique hybrid coordination polymer comprising of a cationic coordination network and anionic covalent chains. The elastomer returned to **1a** upon heating. The application of light and heat resulted in a coordination structure transformation that caused reversible changes in viscoelasticity and ionic conductivity. The liquid **1a** was synthesized by polymerization of ionic liquid **1b** containing an $H_2C{=}CHSO_2NSO_2CF_3^-$ anion. UV photoirradiation transformed **1b** into a viscous elastomer **2b** consisting of a coordination network, though the elastomer changed into **1a** upon heating via polymerization of the anion.

INTRODUCTION

There are many studies on the synthesis and applications of ionic liquids (ILs), which are salts with a melting point below 100 °C.[1] Their negligible vapor pressure, flame retardancy, and high ionic conductivity are highly beneficial for electrochemical applications. Although most ILs contain organic cations, metal-containing cations or anions can be used to develop ILs with functionalities derived from the metal ions.[2–9] To develop materials that undergo structural transformation by external stimuli, we have synthesized ILs containing photoreactive ruthenium (Ru) sandwich complexes.[10–13] For example, we reported previously that IL **1** (Figure 1) transforms into an amorphous coordination polymer (CP) **2** upon UV photoirradiation.[10] In this reaction, photodissociation of the arene ligand followed by coordination of the cyano group to the Ru center forms the network structure. A reverse reaction occurs upon heating the solid. Based on this mechanism, the reversible control of ionic conductivity and viscoelasticity by the application of light and heat was realized.[11]

Poly(ionic liquid)s (PILs) are ionically conductive polymers synthesized by the polymerization of ILs with polymerizable substituents.[14–17] They are versatile because they

display both the characteristics of ILs and polymers, though the development of stimuli-responsive poly(ionic liquid)s is limited. In this study, to develop photoresponsive PILs, we introduced a polymeric anion into **1** (Figure 2a). We hypothesized that its photoreaction would produce a novel hybrid CP containing both covalent chains and coordination networks. Bonding transformation or reorganization of polymers by external stimuli attracted much attention recently, as documented by self-healing polymers,[18] Ru-containing polymers,[19,20] photoresponsive polymers,[21,22] and high-strength gels.[23] Furthermore, the development of photocontrollable soft ionic conductors is an important topic of investigation. There are currently only a few examples of such materials,[24–28] most of which contain photochromic moieties.

This article reports the synthesis, properties, and reactivities of PIL **1a** and its precursor IL **1b** (Figure 2), which have the same cations as **1**. UV photoirradiation transformed PIL **1a** into a unique amorphous hybrid CP via the formation of a coordination network between the cations, and the reaction was reversed by heating. Similarly, UV photoirradiation transformed IL **1b** into an amorphous CP but heating the product unexpectedly produced PIL **1a** via polymerization of the anion. The physical properties of these materials were investigated by differential scanning calorimetry (DSC) and dynamic rheological measurements. Furthermore, we demonstrate that their ionic conductivities are controlled by the application of light and heat based on the bonding transformation mechanism.

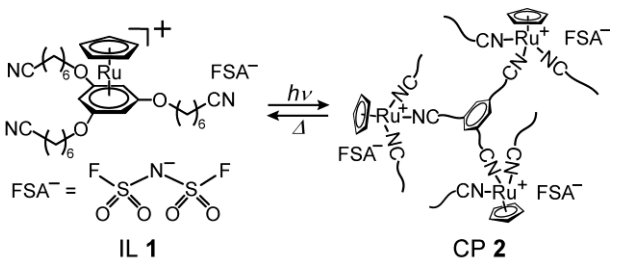

Figure 1. Reversible transformation between metal-containing IL **1** and amorphous CP **2**. The methylene chains of the coordination polymer have been omitted for simplicity.

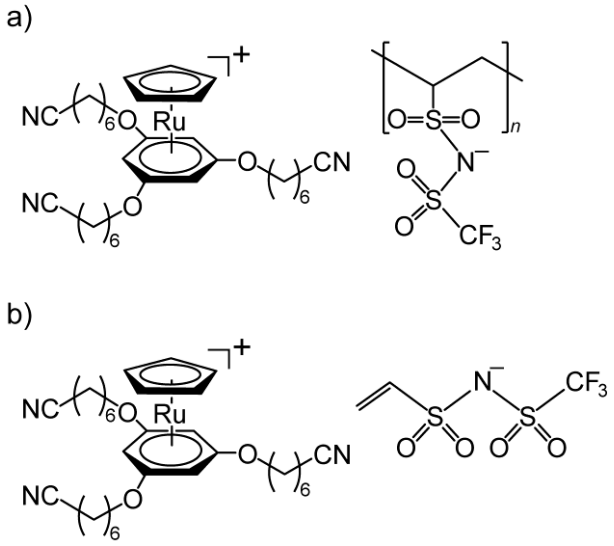

Figure 2. Structural formulae of (a) poly(ionic liquid) **1a** and (b) polymerizable ionic liquid **1b**.

EXPERIMENTAL SECTION

General. $[Ru(Cp)\{1,3,5\text{-}C_6H_3(OC_6H_{12}CN)_3\}][PF_6]$ was synthesized according to a literature method.[10] $K[H_2C{=}CHSO_2NSO_2CF_3]$ was synthesized by the method found in the literature but slightly modified.[29] Water was used instead of saturated $NaHCO_3$ aq. to wash the dichloromethane solution of the precursor $NHEt_3$ salt. ^1H and ^{19}F NMR spectra were recorded on a Bruker Avance 400 MHz spectrometer. FT-IR spectra were acquired via attenuated total reflectance (ATR) using a Thermo Scientific Nicolet iS5 spectrometer. UV–Vis spectra were obtained with a JASCO V-570 UV/VIS/NIR spectrophotometer. DSC measurements were performed using a TA Instrument Q100 differential scanning calorimeter at a scan rate of 10 °C min^{-1}. Thermogravimetric analyses were performed under a nitrogen atmosphere at a heating rate of 5 °C min^{-1} on a Rigaku TG8120 thermogravimetric analyzer. Dynamic viscoelasticities

were measured using a TA Instruments DHR-2 rheometer equipped with an 8 mm parallel plate. The frequency dependence of the dynamic viscoelasticities was established at 25 °C under an application of 1% strain. Ionic conductivities were determined using a Solartron 1260 impedance analyzer. Gold interdigitated electrodes with gap dimensions of 200 μm were used, and the cell constant assessed by measuring the conductivity of 0.01 M KCl aqueous solution at 25 °C. The molecular weight and molecular weight distribution (M_w/M_n) were determined by gel permeation chromatography/size exclusion chromatography (GPC/SEC) on a TOSOH HLC-8320GPC system. Two TSKgel SuperAWM-H (6.0 mm I.D. × 15 cm) columns were used and *N*, *N*-dimethylformamide (DMF) containing 10 mM LiBr was used as the eluent (flow rate 0.6 mL/min, 40 °C). Linear polystyrene standards (Tosoh) in the range of 5.89×10^2 to 5.48×10^6 g mol^{-1} were used for calibration.

Synthesis of ionic liquid 1b. A solution of [**1**][PF_6] (168 mg, 0.22 mmol) in a mixture of acetonitrile (1 mL) and methanol (10 mL) was charged to an anion exchange column (Dowex 1X8-100, chloride form, 7 g), and eluted with methanol (100 mL). The eluent was concentrated using a rotary evaporator, and the anion exchange performed again. The solvent was evaporated under reduced pressure at room temperature to quantitatively obtain [**1**]Cl as a colorless liquid. K[H_2C=$CHSO_2NSO_2CF_3$] (181 mg, 0.65 mmol) was added to a dichloromethane dispersion (15 mL) of [**1**]Cl (143 mg, 0.22 mmol) and stirred for 1 h. An excess amount of the potassium salt was used because the anion exchange was carried out in the dispersion state. To this solution, water (10 mL) was added and the solution further stirred for 1 h. The water layer was removed with a pipette, and the organic layer was washed five times with water and dried over anhydrous magnesium sulfate. The solvent was separated using a rotary evaporator at room temperature, and the residue was dissolved in dichloromethane and charged to a short plug of alumina placed in a chromatography column. After eluting impurities (R_f = 1.0) with dichloromethane/acetonitrile (4:1 v/v), acetonitrile was used to elute the desired product. The

solvent was evaporated at room temperature to give the product as a pale yellow liquid, which was further dried under vacuum at ambient temperature for 1 day (yield 138 mg, 74%). An aqueous solution of silver nitrate was used to check the absence of chloride ion. ^{1}H NMR (400 MHz, $(CD_3)_2CO$): δ = 1.52 (m, 12H, CH_2), 1.68 (m, 6H, CH_2), 1.82 (m, 6H, CH_2), 2.49 (t, 6H, CH_2, J = 6.9 Hz), 4.15 (t, 6H, CH_2, J = 6.3 Hz), 5.46 (s, 5H, Cp-H_5), 5.57 (dd, 1H, *cis*-CH, J = 0.76, 10.0 Hz), 5.94 (dd, 1H, *trans*-CH, J = 0.7, 16.7 Hz), 6.38 (s, 3H, Ar-H_3), 6.80 (dd, 1H, CHSO$_2$, J = 9.9, 16.6 Hz). ^{19}F NMR (400 MHz, $(CD_3)_2CO$): δ = –78.79 (s, 3F, CF_3). Anal. Calcd. for $C_{35}H_{47}F_3N_4O_7RuS_2$: C, 49.00; H, 5.52; N, 6.53. Found: C, 48.85; H, 5.46; N, 6.39. FT-IR (ATR, cm^{-1}): 605, 794, 966 (C=C), 1049 (S=O), 1124, 1172 (S=O), 1321 (S=O), 1414, 1465, 1533 (Ar, C–C), 1632 (C=C), 2244 (CN), 2865 (C–H), 2938 (C–H).

Synthesis of poly(ionic liquid) 1a. The mixture of **1b** (65 mg, 7.6 × 10^{-2} mmol) and AIBN (0.6 mg, 3.7 × 10^{-3} mmol) was heated at 100 °C for 4 days in the dark under a nitrogen atmosphere. The resulting black viscous liquid was dissolved in a small amount of dichloromethane. The desired product was precipitated by adding a large amount of diethyl ether, and the supernatant removed with a pipette. This procedure was repeated three times to produce an orange yellow highly viscous liquid (yield 57 mg, 88%). ^{1}H NMR spectra ($(CD_3)_2SO$) confirmed that the monomer content was less than 3%. The polymerization reaction hardly proceeded when performed in methanol or DMF, hence we adopted the bulk polymerization. However, the bulk polymerization at 70°C for 3 days left 20% of the monomer unreacted. ^{1}H NMR (400 MHz, $(CD_3)_2SO$): δ = 1.42 (m, 12H, CH_2), 1.59 (m, 6H, CH_2), 1.68 (m, 6H, CH_2), 2.33 (br, 6H, CH_2), 3.97 (t, 6H, CH_2, J = 5.9 Hz), 5.13 (s, 5H, Cp-H_5), 6.34 (s, 3H, Ar-H_3). ^{19}F NMR (400 MHz, $(CD_3)_2SO$): δ = –77.55 (s, 3F, CF_3, head to head), –77.53 (s, 3F, CF_3, head to tail). FT-IR (ATR, cm^{-1}): 605, 794, 1048 (S=O), 1123, 1171 (S=O), 1320 (S=O), 1414, 1465, 1533 (Ar, C–C), 2244 (CN), 2865 (C–H), 2938 (C–H). The molecular weights of PIL **1a** relative to polystyrene standards as determined by GPC/SEC with DMF

containing LiBr as the eluent were $M_w = 4.85 \times 10^3$ g mol^{-1}, $M_n = 4.2 \times 10^3$ g mol^{-1}, and M_w/M_n = 1.16 (Figure S10).

Investigations of reactivities. The UV photoirradiation of the liquids was performed at 10 °C using a Lightningcure UV-LED spotlight source LC-L1V5 (365 nm, 600 mW cm^{-2}). The liquid samples were sandwiched between two quartz plates. The photoirradiation of the samples to measure the ionic conductivity was conducted using sealed electrodes. Thermal reactions were performed using a preheated oven at 120 °C. The dissociation rates of the cation in the photoproducts were determined from the ratio of $[Ru(C_5H_5)(NCCD_3)_3]^+$ and the remaining sandwich complex in the ^{1}H NMR spectra in CD_3CN.

RESULTS AND DISCUSSION

Synthesis and reactivities of PIL 1a and IL 1b. PIL **1a** is an orange-yellow highly viscous liquid, which was synthesized by bulk polymerization of IL **1b** in the presence of azobisisobutyronitrile (AIBN) in 88% yield. IL **1b** is a pale yellow liquid, synthesized by the anion exchange of the corresponding chloride salt (yield 74%). The thermal decomposition temperature of IL **1b** as determined by thermogravimetric analysis was 201 °C (−3wt% weight loss temperature, Figure S1). PIL **1a** and IL **1b** exhibited glass transitions at −43 and −52 °C, respectively, as determined by DSC (Table 1). It is reasonable that the PIL exhibits a higher glass transition temperature than the IL.[30] The comparable glass transition temperature of ILs **1b** and **1** (T_g = −53 °C[10]) seems reasonable considering their similar molecular structures.

An overview of the photochemical and thermal reactivities of these materials is shown in Figure 3. PIL **1a** formed a cationic network upon UV photoirradiation, transforming into an amorphous hybrid CP **2a** in a few hours. Similarly, IL **1b** transformed into an amorphous CP **2b** upon photoirradiation. In these reactions, some unreacted cations remained in the resultant solids. CPs **2a** and **2b** exhibited glass transitions at −8 °C and −21 °C, respectively,

temperatures that are higher than those of **1a** and **1b**. The higher glass transition temperature of CP **2a** compared to that of CP **2b** is ascribed to the anionic polymer chains in **2a**. CP **2a** changed back to PIL **1a** upon heating. However, CP **2b** did not form IL **1b** but was transformed into PIL **1a** upon heating via polymerization of the anion's functional group. The details of each reaction are discussed in the following sections.

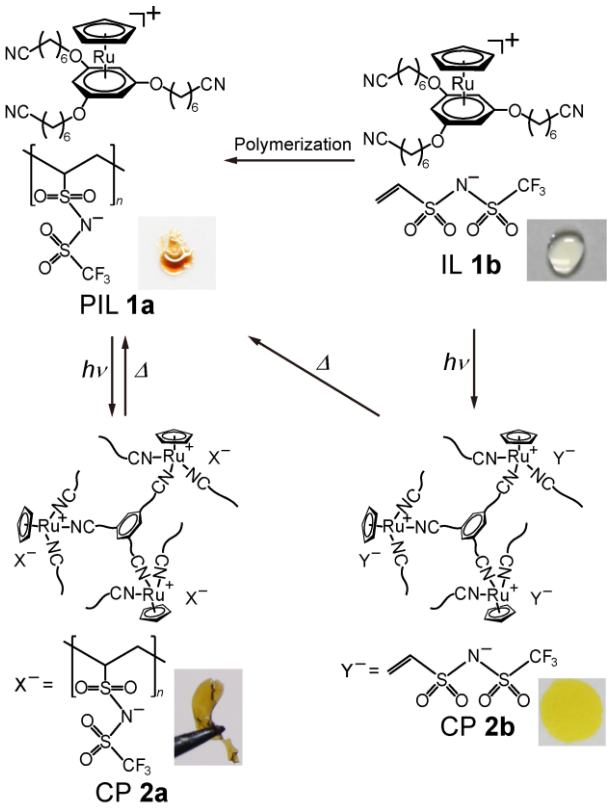

Figure 3. Photochemical and thermal reactions of PIL **1a** and IL **1b**. Anions X^- and Y^- are polymeric and polymerizable anions, respectively. The methylene chains of the coordination polymer have been omitted for simplicity. The photograph of CP **2b** is of the sample sandwiched between quartz plates.

Table 1. Glass Transition Temperatures of PILs, IL, and CPs

compound	T_g (°C)
1a (PIL)	–43
1b (IL)	–52
1[a] (IL)	–53
2a (CP, 69%)[b]	–8
2b (CP, 92%)[b]	–21
2[a] (CP, 100%)[b]	0

[a]Ref. 10. [b]Reaction rates are shown in parenthesis.

Photochemical reactivity of PIL 1a. Upon UV photoirradiation, the orange-yellow highly viscous liquid PIL **1a** gradually transformed into the orange rubbery elastomer **2a** (Figure 3, left), via the formation of a cationic network structure. Heating the elastomer caused a reverse reaction to generate liquid **1a**. This transformation was reversibly repeated in an Ar atmosphere but became gradually irreversible in air owing to oxidation.

The elastomer **2a** generated by photoirradiation of PIL **1a** is an amorphous hybrid CP, comprising of anionic covalent chains and a cationic coordination network. Consistently, this photochemical reaction was accompanied by shifts in C=C stretching vibrations from 1532 to 1593 cm^{-1} and CN stretching vibrations from 2245 to 2272 cm^{-1} in the FT-IR spectrum and an increase in absorption around 310 and 370 nm in the UV–Vis spectrum (Figures 4 and S2). They correspond to the structural transformation from the sandwich complex to the cyano-coordinated complex.[10,31] The reaction rate, or cation dissociation rate after photoirradiation for 4 h was 75% as determined from ^{1}H NMR spectra in CD_3CN (Figure S3). Prolonged photoirradiation did not increase the reaction rate. Therefore, 25% of the Ru complexes remained in the product as the sandwich complex, which percentage did not decrease upon

further photoirradiation. The presence of residual sandwich complexes (~20%) is also observed in the photoreaction product of **1**, which is ascribed to the incorporation of unreacted molecules into the network during photoreaction.[10]

CP **2a** returned to PIL **1a** upon heating at 90 °C for 2h. However, the reaction rate was 95%, and 5% of the cyano-coordinated complex remained in the liquid. The thermal reaction was further investigated by DSC (Figure 5). In the heating process, CP **2a** showed a glass transition at −8 °C and a very broad endothermic peak at 70–140 °C (ΔH = 4 kJ mol^{-1}, peak top 105 °C), which relates to the conversion to PIL **1a**. This is consistent with CP **2** showing a broad endothermic peak (ΔH = 5.2 kJ mol^{-1}) at 50–120 °C upon transformation to IL **1**.[10] The reaction enthalpy of CP **2a** corresponds to approximately 70% of that of **2**, which is consistent with the reaction rate of the cation (75%). In the second cycle, a glass transition was observed at −39 °C, which also indicates the formation of PIL **1a**. The slightly higher glass transition temperature than that of the original **1a** (T_g = −43 °C) resulted from the low reaction rate of the cation (85%) owing to the shorter heating time.

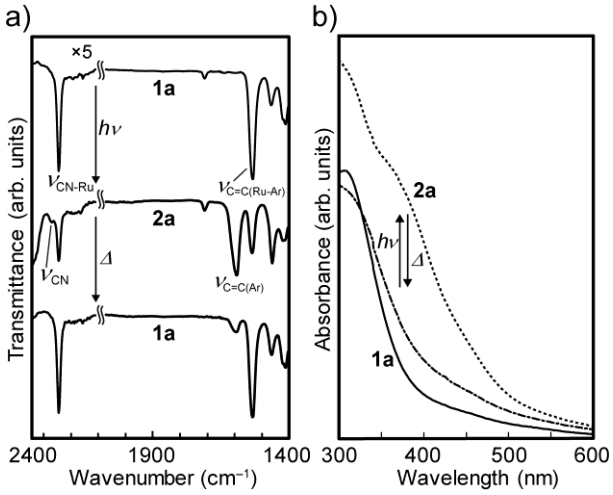

Figure 4. (a) FT-IR spectra and (b) UV–vis spectra of PIL **1a**, CP **2a**, and after heating **2a** at 90 °C for 2 h.

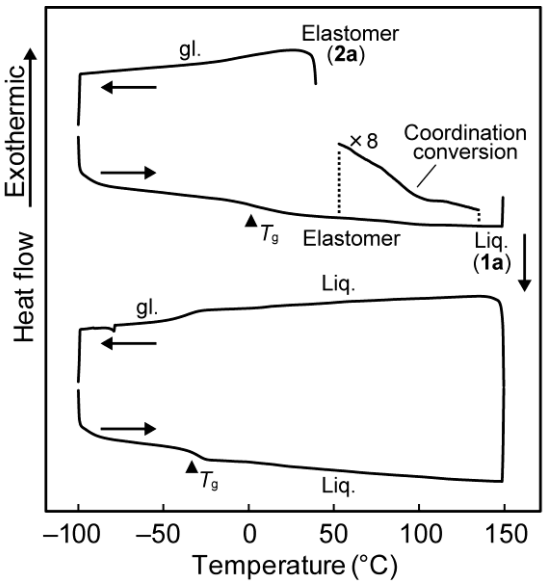

Figure 5. DSC traces of CP **2a**, where liq. and gl. are the liquid and glassy states, respectively.

Photochemical reactivity of IL 1b. Upon UV photoirradiation, the pale yellow liquid **1b** converted into the amorphous CP **2b**, which was an orange viscous elastomer. The product was not changed back to **1b** upon heating but transformed into PIL **1a** (Figure 3) via polymerization of the anion. Therefore, a reversible transformation between PIL **1a** and CP **2a** was observed in the subsequent alternate cycles of photoirradiation and heating.

The elastomer **2b** generated by UV photoirradiation of IL **1b** is an amorphous CP with a cationic network structure (Figure 3, right). The formation of the cyano-coordinated structure was also confirmed by UV–vis and FT-IR spectra (Figure S5). The reaction rate was 95% after UV photoirradiation for 4 h, and 5% of the sandwich complex remained in the product (Figure S6). Further photoirradiation did not increase the reaction rate.

CP **2b** transformed into PIL **1a** upon heating, not shifting back to IL **1b**. Heating caused polymerization of the anion concomitant with the structural transformation of the cations. The cations switched back to the sandwich complex almost quantitatively (98%) upon heating at 120 °C for 12 h, whereas 92% of anions were polymerized. At a milder condition of heating at

90 °C for 2 h, 91% of the cations changed back to the sandwich complex and 57% of anions polymerized. The uncommon anion polymerization is owing to the catalytic activity of the Ru half-sandwich complex. This was proven by heating the mixture of **1b** and a half-sandwich complex $[Ru(Cp)(NCCH_3)_3][PF_6]$ at 90 °C, which produced the polymerized anion in 7 mol% in 2 h, whereas heating **1b** alone did not cause any reactions. It is noteworthy that the constituent of the CP itself acted as a catalyst.

The thermal reaction of CP **2b** to PIL **1a** was investigated by DSC (Figure S7). Upon heating, **2b** exhibited a glass transition at −21 °C, and a very broad endothermic peak was observed at 40–100 °C owing to the coordination transformation of the cation, overlapped with subsequent exothermic polymerization of the anion. In the second cycle, a glass transition was observed at −43 °C, which is consistent with T_g of **1a**. After the DSC measurement, the cations in the sample changed back to the sandwich complex almost quantitatively (97%) and 66% of the anions were polymerized.

Dynamic viscoelasticity. Dynamic viscoelasticity measurements were performed at 25 °C to evaluate the changes in mechanical properties of PIL **1a** and IL **1b** upon photoirradiation. Photoirradiation caused a marked increase in viscoelasticity owing to the transformation to CP. The samples after photoirradiation of **1a** for 20 h (65% reaction rate) and that of **1b** for 8 h (77%) are designated in this section as **2a** and **2b**, respectively. Their reaction rates were lower than those reported in the previous sections because the samples were thicker.

The elastic moduli and complex viscosities of these materials at an angular frequency of 10 rad s^{-1} are summarized in Table 2 together with those of **1** and **2**. The viscosities at a shear rate of 1 s^{-1} are also shown in the table. The viscosities of **1a**, **1b**, and **1** were 1.3×10^2 Pa s (1.3×10^5 cP), 7.7 Pa s (7.7×10^3 cP), and 2.6 Pa s (2.6×10^3 cP), respectively. Therefore, PIL **1a** was much more viscous than ILs **1b** and **1**. Similarly, the storage modulus of **1a** (1.9×10^2 Pa) was much larger than those of **1b** (11.1 Pa) and **1** (9.4 Pa). The higher values for the PIL

compared to ILs and comparable values for ILs **1b** and **1** are reasonable considering their similar molecular structures. All the values increased markedly after photoirradiation. The storage modulus of **2a** and **2** increased compared to those of **1a** and **1** by orders of 10^4 and 10^5, respectively, whereas the increase from **1b** to **2b** was smaller in the order of 10^2. The loss modulus and complex viscosity of each liquid increased similarly. The elastic moduli of the photoproducts decreased in the order of **2a** (~10^6 Pa) > **2** (~10^5 Pa) > **2b** (~10^3 Pa). This trend is consistent with their physical appearance as rubbery, soft, and viscous elastomers, respectively. Furthermore, there was a correlation between the complex viscosities and glass transition temperatures (Table 1), both decreased in the order of **1a** > **1b** > **1**.

The angular frequency dependence of the storage modulus G' and loss modulus G'' of PIL **1a** measured at 1% strain before and after UV photoirradiation is shown in Figure 6a. In **1a**, G'' exceeds G' in the entire frequency range, indicating viscous behavior (tan δ> 1). The slopes of G' and G'' of PIL **1a** in the range of 10^2–10^3 rad s^{-1} were 2 and 1, respectively, which is a typical behavior in the terminal region.[32] However, the slope of G' was smaller below 10^2 rad s^{-1}, which is probably ascribed to the formation of domains owing to the interactions between constituent ions.[33,34] Both G'' and G' improved upon photoirradiation and increased by more than three orders of magnitude in 20 h. In CP **2a**, G' exceeded G'' (tan δ< 1) at around 400 rad s^{-1}, indicating elastic behavior. The oscillation strain dependence of viscoelasticity at this angular frequency confirmed the elastic behavior, though structural failure occurred at 2% strain (Figure S8). The region below 400 rad s^{-1} corresponds to the glass–rubber transition region for this material.[32] The angular frequency dependence of the complex viscosity of **1a** before and after photoirradiation is shown in Figure 7. The complex viscosities increased by three orders of magnitude upon photoirradiation. The shear rate dependence of the viscosities of **1a** and **2a** are shown in the inset of Figure 7. **2a** exhibited a sharp decrease in viscosity at a shear rate above 10 s^{-1}, which indicates a structural failure.

Similar to PIL **1a**, the elastic moduli of IL **1b** increased upon photoirradiation (Figure 6b). The loss modulus (G'') exceeds the storage modulus (G') before photoirradiation, showing viscous behavior. After photoirradiation for 4 and 8 h, G' exceeded G'' in the angular frequency range below 10 and 3 rad s^{-1}, respectively, indicating elastic behavior in these regions. The low-frequency shift of the intersection of G' and G'' (tan $\delta = 1$) with increasing photoirradiation period is ascribed to the shift of the glass–rubber transition region owing to the increase of the glass transition temperature.[32] The viscosity of the liquid also exhibited a large increase upon photoirradiation (Figure S9). Both IL **1b** and CP **2b** displayed Newtonian behavior. It is noteworthy that, though **1b** and **2b** are structurally similar to **1** and **2**, significant differences were observed in their viscoelasticities. The viscosity of **1b** was similar to that of **1**, but the storage modulus of **1b** revealed a more significant angular frequency dependence than **1**. The storage modulus of **2b** (~10^3 Pa) was much smaller than that of **2** (~10^5 Pa, Table 2).

As shown, the investigation of the viscoelastic changes of PIL **1a** and IL **1b** upon photoirradiation demonstrated their transformation to elastomers. In particular, the presence of anionic polymer chains considerably enhances the elastic modulus and viscosity, and the different molecular structures resulted in a significant variance in their viscoelastic properties.

Table 2. Storage and Loss Modulus, Complex Viscosity, and Viscosity of the Samples at 25 °C

Compound	Storage modulus (Pa)[c]	Loss modulus (Pa)[c]	Complex viscosity (Pa s)[c]	Viscosity (Pa s)[d,e]
1a (PIL)	1.9×10^2	1.3×10^3	1.3×10^2	1.3×10^2
1b (IL)	1.1×10^1	1.1×10^2	6.5	7.7
1[a] (IL)	9.4	2.9×10^1	3.0	2.6
2a (CP, 65%)[b]	1.3×10^6	1.7×10^6	2.1×10^5	1.0×10^5
2b (CP, 77%)[b]	2.5×10^3	8.2×10^3	8.6×10^2	7.3×10^2
2 [a] (CP, 55%)[b]	4.7×10^5	2.0×10^5	5.1×10^4	

[a]Ref 11. [b]Reaction rate is shown in parenthesis. [c]Value at an augular frequency of 10 rad s^{-1}. [d]Value at a shear rate of 1 s^{-1}. [e]1 Pa·s = 10^3 cP.

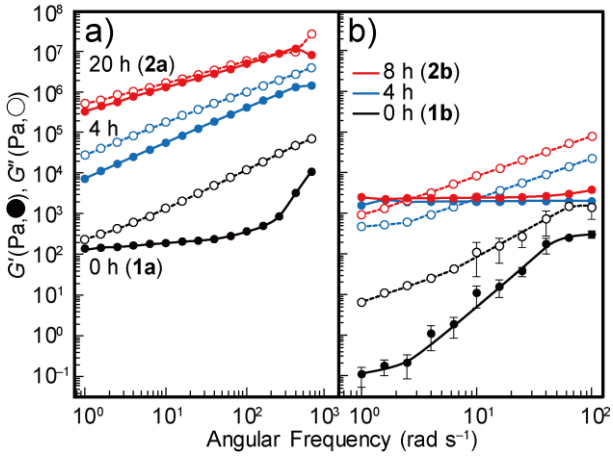

Figure 6. Angular frequency dependence of storage moduli (●) and loss moduli (○) of (a) PIL **1a** and (b) IL **1b** before and after photoirradiation (1% strain).

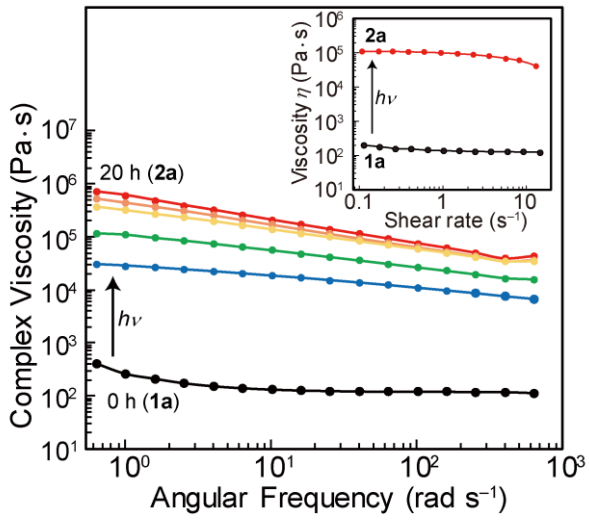

Figure 7. Complex viscosity of PIL **1a** before and after UV photoirradiation determined at 4 h intervals (1% strain). The inset shows the shear rate dependence of the viscosities of PIL **1a** and CP **2a**.

Ionic conductivity. The ionic conductivities of PIL **1a** and IL **1b** before and after photoirradiation were measured at 25 °C (Table 3). The ionic conductivity markedly decreased upon photoirradiation, a result of the decreased mobility of the cations. The ionic conductivity was controllable by the application of light and heat.

The ionic conductivities of **1a** and **1b** were 2.2×10^{-6} and 1.9×10^{-5} S cm^{-1}, respectively. The lower value of **1a** is due to the polymeric anion, whereas the ionic conductivity of **1b** is comparable to that of **1** (3.1×10^{-5} S cm^{-1}). These ionic conductivities are considerably lower than those of common ionic liquids ([Bmim][Tf_2N]: 4.1×10^{-3} S cm^{-1} at 25 °C[35]) with respect to their high viscosity. However, the value of the ionic conductivity of **1a**, which contains a small amount of monomer **1b** (< 3 mol%), should be taken with care, because the presence of 3wt% of residual ionic monomer may double the conductivity of the resultant polymer.[36] The Walden product, the product of ionic conductivity and solution viscosity, of **1b** is approximately 10^{-1} mPa s S cm^{-1}, which is comparable to those of common ionic liquids.[37,38]

The ionic conductivity of **1a** gradually decreased upon photoirradiation, decreasing by one order of magnitude in 1 h (Figure 8a). Heating the photoirradiated sample at 120 °C for 20 min increased the conductivity, hence the ionic conductivity was reversibly controlled by the alternate application of light and heat (Figure 8b, left). Photoirradiation for more than 1 h decreased the ionic conductivity further, but a precise value could not be determined because of instrumental limitations. On the other hand, **1b** has a higher ionic conductivity than **1a** and photoirradiation for 1 h decreased its ionic conductivity by 2 orders of magnitude (Figure 8a, dotted curve). Heating the photoproduct at 120 °C for 1 h increased the conductivity by 1 order of magnitude (Figure 8b, right). The initial value was not obtained because the product was **1a**, as shown in the previous section. Hence, the subsequent alternate application of light and heat caused a reversible transformation between **1a** and its photoproduct, which resulted in the reversible ionic conductivity change (Figure 8b, right). The better repeatability of the ionic conductivity variation starting from **1b** (Figure 8b, right) than **1a** (Figure 8b, left) may be ascribed to the lower viscosity of **1b**, providing better contact with the electrodes.

These results demonstrated that the ionic conductivities of these materials can be controlled by the application of light and heat. Several polymers,[24–26] ILs,[11,27] and PILs[28] exist that exhibit reversible control of ionic conductivity by photoirradiation, though most of them are based on photochromic molecules and few involved in bonding transformation.[11,24,25] As demonstrated in the present and previous studies,[11] the photochemical immobilization of ions enables a direct and flexible control of the ionic conductivity, which should be beneficial for various applications.

Table 3. Ionic Conductivity (25 °C) and Walden Product of 1a, 1b, and 1

Compound	Ionic conductivity (S cm^{-1})		Walden product
	Before	After 1h irradiation	(mPa s S cm^{-1})
1a	2.2×10^{-6}	2.0×10^{-7}	–
1b (1^{st} cycle)	1.9×10^{-5}	3.2×10^{-7}	1.5×10^{-1}
(2^{nd} cycle)[a]	3.1×10^{-6}	3.0×10^{-7}	–
1[b]	3.1×10^{-5}	4.8×10^{-7} [c]	8.1×10^{-2}

[a]Transformed to **1a**. [b]Ref. 11. [c]After 2 h of photoirradiation.

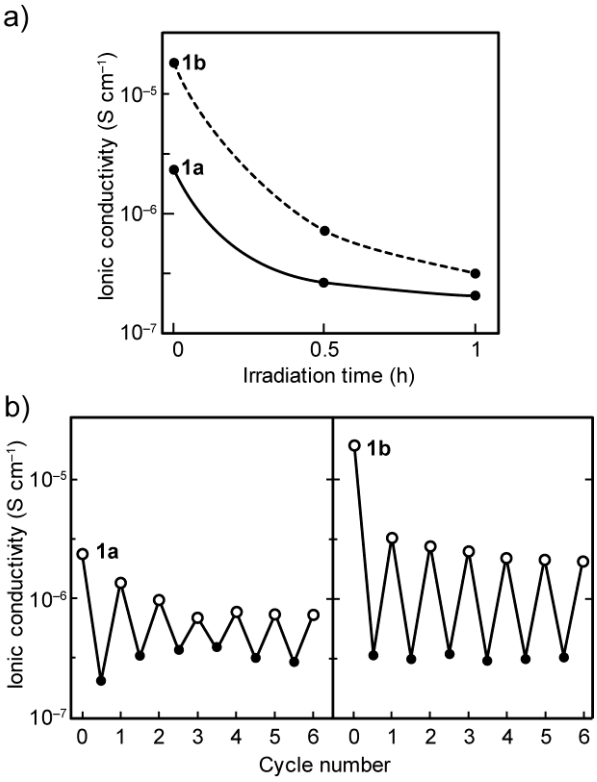

Figure 8. Ionic conductivities of PIL **1a** and IL **1b** at 25 °C. (a) Time course of ionic conductivities upon UV photoirradiation. (b) Ionic conductivity changes for alternating cycles of UV photoirradiation for 1 h (filled circles) and heating at 120 °C for 20 min (open circles). The heating period was 1 h only in the first cycle of **1b**.

CONCLUSION

In this study, we developed a Ru-containing PIL whose viscoelasticity and ionic conductivity can be reversibly controlled by photochemical and thermal reactions. This PIL transformed to an amorphous hybrid CP upon UV photoirradiation, and a reverse reaction occurred upon heating. Furthermore, the precursor IL of this PIL similarly transformed to an amorphous CP upon photoirradiation. Heating the elastomer produced the PIL, owing to the catalytic activity of the cation. The resulting elastomer from the PIL is a hybrid CP comprising anionic covalent chains and a cationic coordination network. The mechanical properties of the unique polymer warrant further investigation.

In these materials, the ionic conductivity can be controlled by the application of light and heat, the result of the reversible immobilization of the cations. The nonvolatility and high ionic conductivity of PILs and ILs are advantageous properties for photocontrollable electronic and photoresist materials. The strategy followed in this study can be extended to the design of photoresponsive gels and membranes, studies of which are presently being conducted in our laboratory.

ASSOCIATED CONTENT

Supporting Information.

NMR, FT-IR, UV–Vis spectra, DSC traces, and rheological data. This material is available free of charge via the Internet at http://pubs.acs.org.

AUTHOR INFORMATION

Corresponding Author

*E-mail: tmochida@platinum.kobe-u.ac.jp

ORCID

Tomoyuki Mochida: 0000-0002-3446-2145

Notes

The authors declare no competing financial interest.

ACKNOWLEDGMENTS

This work was supported financially by the Canon foundation and KAKENHI (20H02756 and 18H04516) from the Japan Society for the Promotion of Science (JSPS). We thank the anonymous reviewers for their useful comments.

REFERENCES

(1) Kar, M.; Matuszek, K.; MacFarlane, D. R. Ionic Liquids. *Kirk–Othmer Encyclopedia of Chemical Technology*; John Wiley & Sons, Inc., **2020**, doi:10.1002/0471238961.ionisedd.a01.pub2

(2) Brooks, N. R.; Schaltin, S.; Van Hecke, K.; Van Meervelt, L.; Binnemans, K.; Fransaer, J. Copper(I)-Containing Ionic Liquids for High-Rate Electrodeposition. *Chem. - Eur. J.* **2011**, *17*, 5054–5059.

(3) Iida, M.; Baba, C.; Inoue, M.; Yoshida, H.; Taguchi, E.; Furusho, H. Ionic Liquids of Bis(alkylethylenediamine)silver(I) Salt

s and the Formation of Silver(0) Nanoparticles from the Ionic Liquid System. *Chem. - Eur. J.* **2008**, *14*, 5047−5056.

(4) Branco, A.; Branco, L. C.; Pina, F. Electrochromic and Magnetic Ionic Liquids. *Chem. Commun.* **2011**, *47*, 2300−2302.

(5) Zhang, P.; Gong, Y.; Lv, Y.; Guo, Y.; Wang, Y.; Wang, C.; Li, H. Ionic Liquids with Metal Chelate Anions. *Chem. Commun.* **2012**, *48*, 2334−2336.

(6) Yoshida, Y.; Saito, G. Progress in Paramagnetic Ionic Liquids. In *Ionic Liquids: Theory, Properties, New Approaches*; Kokorin, A., Ed.; IntechOpen: 2011; pp 723−738.

(7) Tominaga, T.; Mochida, T. Multifunctional Ionic Liquids from Rhodium(I) Isocyanide Complexes: Thermochromic, Fluorescence, and Chemochromic Properties Based on Rh-Rh Interaction and Oxidative Addition. *Chem. - Eur. J.* **2018**, *24*, 6239−6247.

(8) Lan, X.; Mochida, T.; Funasako, Y.; Takahashi, K.; Sakurai, T.; Ohta, H. Thermochromic Magnetic Ionic Liquids from Cationic Nickel(II) Complexes Exhibiting Intramolecular Coordination Equilibrium. *Chem. - Eur. J.* **2017**, *23*, 823−831.

(9) Inagaki, T.; Mochida, T.; Takahashi, M.; Kanadani, C.; Saito, T.; Kuwahara, D. Ionic Liquids of Cationic Sandwich Complexes. *Chem. - Eur. J.* **2012**, *18*, 6795−6804.

(10) Funasako, Y.; Mori, S.; Mochida, T. Reversible Transformation between Ionic Liquids and Coordination Polymers by Application of Light and Heat. *Chem. Commun.* **2016**, *52*, 6277−6279.

(11) Sumitani, R.; Yoshikawa, H.; Mochida, T. Reversible Control of Ionic Conductivity and Viscoelasticity of Organometallic Ionic Liquids by Application of Light and Heat. *Chem. Commun.* **2020**, *56*, 6189–6192.

(12) Fan, R.; Sumitani, R.; Mochida, T. Synthesis and Reactivity of Cyclopentadienyl Ruthenium(II) Complexes with Tris(alkylthio)benzenes: Transformation between Dinuclear and Sandwich-Type Complexes. *ACS Omega* **2020**, *5*, 2034–2040.

(13) Ueda, T.; Tominaga, T.; Mochida, T.; Takahashi, K.; Kimura, S. Photogeneration of Microporous Amorphous Coordination Polymers from Organometallic Ionic Liquids. *Chem. – Eur. J.* **2018**, *24*, 9490–9493.

(14) Shaplov, A. S.; Marcilla, R.; Mecerreyes, D. Recent Advances in Innovative Polymer Electrolytes based on Poly(ionic liquid)s *Electrochim. Acta* **2015**, *175*, 18–34.

(15) Yuan, J.; Mecerreyes, D.; Antonietti, M. Poly(ionic liquid)s: An update. *Prog. Polym. Sci.* **2013**, *38*, 1009–1036.

(16) Yuan, J.; Antonietti, M. Poly(ionic liquid)s: Polymers expanding classical property profiles. *Polymer*, **2011**, *52*, 1469–1482.

(17) Mecerreyes, D. Polymeric ionic liquids: Broadening the properties and applications of polyelectrolytes. *Prog. Polym. Sci*. **2011**, *36*, 1629–1648.

(18) Amaral, A. J. R.; Pasparakis, G. Stimuli responsive self-healing polymers: gels, elastomers and membranes. *Polym. Chem.* **2017**, *8*, 6464–6484.

(19) Zhou, H.; Chen, M.; Liu, Y.; Wu, S. Stimuli-Responsive Ruthenium-Containing Polymers. *Macromol. Rapid Commun.* **2018**, *39*, 1800372.

(20) Teasdale, I.; Theis, S.; Iturmendi, A.; Strobel, M.; Hild, S.; Jacak, J.; Mayrhofer, P.; Monkowius, U. Dynamic Supramolecular Ruthenium-Based Gels Responsive to Visible/NIR Light and Heat. *Chem. - Eur. J.* **2019**, *25*, 9851–9855.

(21) Zhu, C. C.; Ninh, C.; Bettinger, C. J. Photoreconfigurable Polymers for Biomedical Applications: Chemistry and Macromolecular Engineering. *Biomacromolecules* **2014**, *15*, 3474–3494.

(22) Brunsveld, L.; Folmer, B. J. B.; Meijer, E. W.; Sijbesma, R. P. Supramolecular Polymers. *Chem. Rev.* **2001**, *101*, 4071–4097.

(23) Haque, M. A.; Kurokawa, T.; Gong, J. P. Super tough double network hydrogels and their application as biomaterials. *Polymer* **2012**, *53*, 1805–1822.

(24) Wang, H.; Zhu, C. N.; Zeng, H.; Ji, X.; Xie, T.; Yan, X.; Wu, Z. L.; Huang, F. Reversible Ion-Conducting Switch in a Novel Single-Ion Supramolecular Hydrogel Enabled by Photoresponsive Host–Guest Molecular Recognition. *Adv. Mater.* **2019**, *31*, 1807328.

(25) Mochizuki, H.; Nabeshima, Y.; Kitsunai, T.; Kanazawa, A.; Shiono, T.; Ikeda, T.; Hiyama, T.; Maruyama, T.; Yamamoto, T.; Koide, N. Photochemical control of conductivity of polythiophenes with photochromic moieties. *J. Mater. Chem.* **1999**, *9*, 2215–2219.

(26) Tokuhisa, H.; Yokoyama, M.; Kimura, K. Photoinduced switching of ionic conductivity by metal ion complexes of vinyl copolymers carrying crowned azobenzene and biphenyl moieties at the side chain. *J. Mater. Chem.* **1998**, *8*, 889–891.

(27) Ishiba, K.; Morikawa, M.; Chikara, C.; Yamada, T.; Iwase, K.; Kawakita, M.; Kimizuka, N. Photoliquefiable Ionic Crystals: A Phase Crossover Approach for Photon Energy Storage Materials with Functional Multiplicity. *Angew. Chem. Int. Ed.* **2015**, *54*, 1532–1536.

(28) Nie, H.; Schauser, N. S.; Dolinski, N. D.; Hu, J.; Hawker, C. J.; Segalman, R. A.; Read de Alaniz, J. Light-Controllable Ionic Conductivity in a Polymeric Ionic Liquid. *Angew. Chem. Int. Ed.* **2020**, *59*, 5123–5128.

(29) Ho, H. T.; Rollet, M.; Phan, T. N. T.; Gigmes, D. "Michael addition" reaction onto vinyl sulfonyl(trifluoromethylsulfonyl)imide: An easy access to sulfonyl(trifluoromethylsulfonyl)imide-based monomers and polymers. *Eur. Polym. J.* **2018**, *107*, 74–81.

(30) Ohno, H.; Yoshizawa, M.; Ogihara, W. Development of new class of ion conductive polymers based on ionic liquids. *Electrochim. Acta* **2004**, *50*, 255–261.

(31) Gill, T. P.; Mann, K. R. Photochemical properties of the cyclopentadienyl(.eta.6-benzene)ruthenium(II) cation. The synthesis and reactions of a synthetically useful intermediate: the cyclopentadienyltris(acetonitrile)ruthenium(II) cation. *Organometallics* **1982**, *1*, 485–488.

(32) Liu, Y.; Winter, H. H.; Perry, S. L. Linear viscoelasticity of complex coacervates. *Adv. Colloid Interface. Sci.* **2017**, *239*, 46–60.

(33) Chile, L.-E., Mehrkhodavandi, P.; Hatzikiriakos, S. G. Aromatic interactions in aryl-capped polylactides: a thermorheological investigation. *J. Rheol.*, **2017**, *61*, 1137–1148.

(34) Chen, Q.; Bao, N.; Wang, J.-H. H.; Tunic, T.; Liang, S.; Colby, R. H. Linear Viscoelasticity and Dielectric Spectroscopy of Ionomer/Plasticizer Mixtures: A Transition from Ionomer to Polyelectrolyte. *Macromolecules* **2015**, *48*, 8240–8252.

(35) Widegren, J. A.; Saurer, E. M.; Marsh, K. N.; Magee, J. W. Electrolytic conductivity of four imidazolium-based room-temperature ionic liquids and the effect of a water impurity. *J. Chem. Thermodyn.* **2005**, *37*, 569–575.

(36) Shaplov, A. S.; Lozinskaya, E. I.; Ponkratov, D. O.; Malyshkina, I. A.; Vidal, F.; Aubert, P. -H.; Okatova, O. V.; Pavlov, G. M.; Komarova, L. I.; Wandrey, C.; Vygodskii, Y. S. Bis(trifluoromethylsulfonyl)amide based "polymeric ionic liquids": Synthesis, purification and peculiarities of structure-properties relationships. *Electrochim. Acta* **2011**, *57*, 74–90.

(37) Xu, W.; Cooper, E. I.; Angell, C. A. Ionic Liquids: Ion Mobilities, Glass Temperatures, and Fragilities. *J. Phys. Chem. B* **2003**, *107*, 6170–6178.

(38) MacFarlane, D. R.; Forsyth, M.; Izgorodina, E. I.; Abbott, A. P.; Annat, G.; Fraser, K. On the concept of ionicity in ionic liquids. *Phys. Chem. Chem. Phys.* **2009**, *11*, 4962–4967.

Supporting Information

Metal-containing Poly(ionic liquid) Exhibiting Photogeneration of Coordination Network: Reversible Control of Viscoelasticity and Ionic Conductivity†

Ryo Sumitani[a] and Tomoyuki Mochida*[a,b]

[a]*Department of Chemistry, Graduate School of Science, Kobe University, Rokkodai, Nada, Kobe, Hyogo 657-8501, Japan. E-mail: tmochida@platinum.kobe-u.ac.jp*

[b]*Center for Membrane and Film Technology, Kobe University, Rokkodai, Nada, Kobe, Hyogo 657-8501, Japan*

Contents

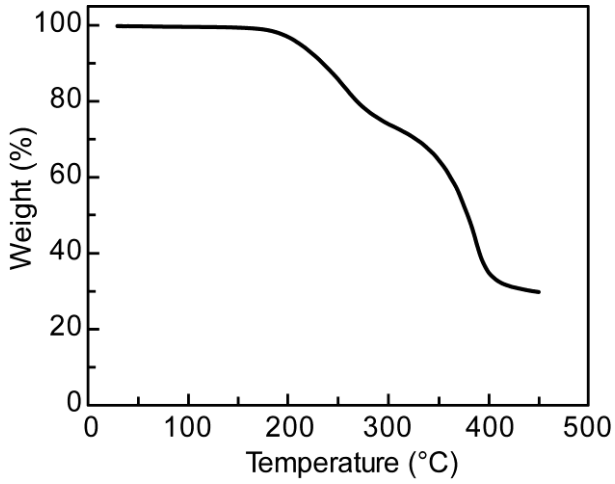

Fig. S1. Thermogravimetric (TG) trace of IL **1b** (heating rate: 5 °C min^{-1}).

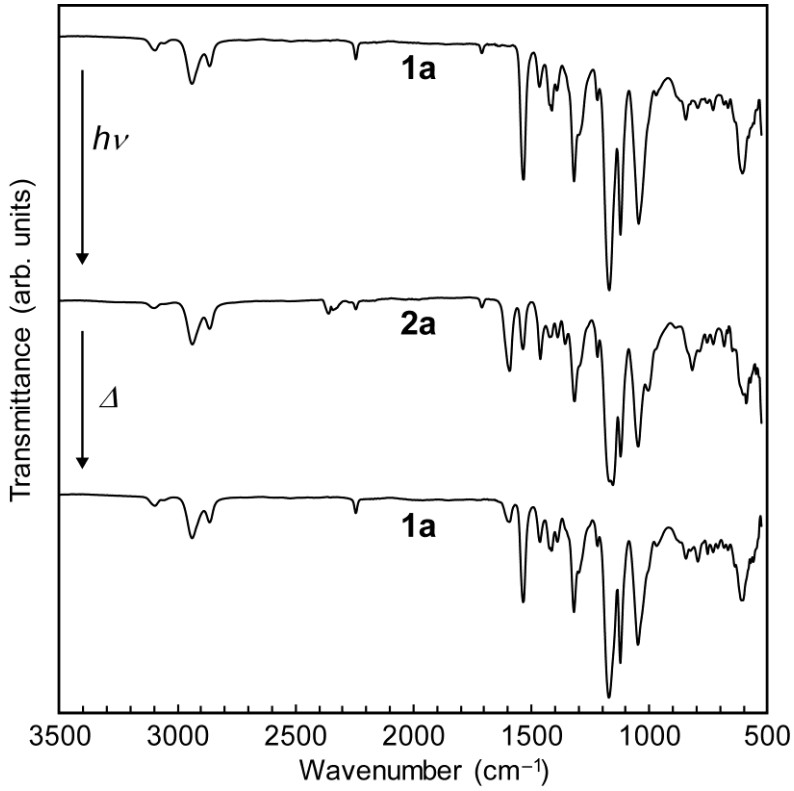

Fig. S2. FT-IR spectra of (a) PIL **1a**, (b) CP **2a**, and (c) after heating **2a** at 90 °C for 2h.

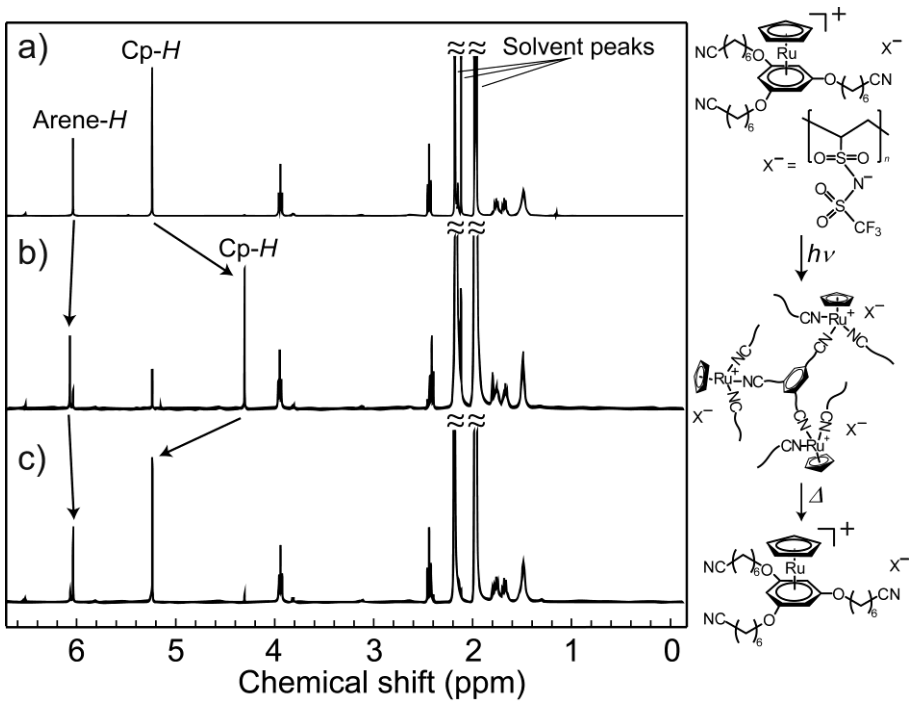

Fig. S3. ^{1}H NMR spectra (400 MHz, CD_3CN) of (a) PIL **1a**, (b) CP **2a**, and (c) after heating **2a** at 90 °C for 2h.

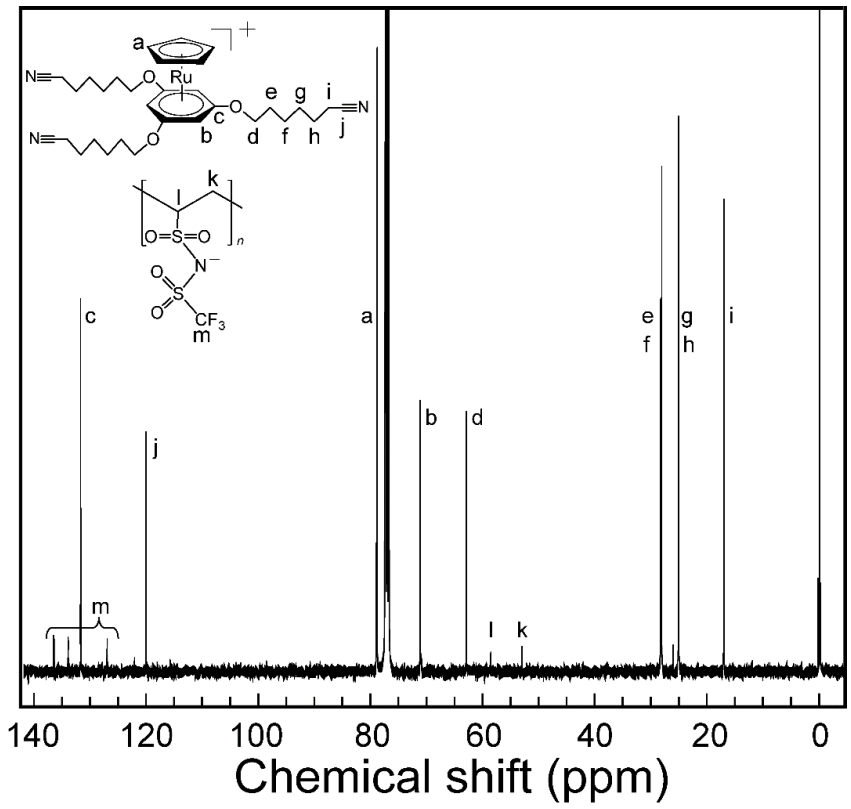

Fig. S4. ^{13}C NMR spectra (100 MHz, $CDCl_3$) of PIL **1a**.

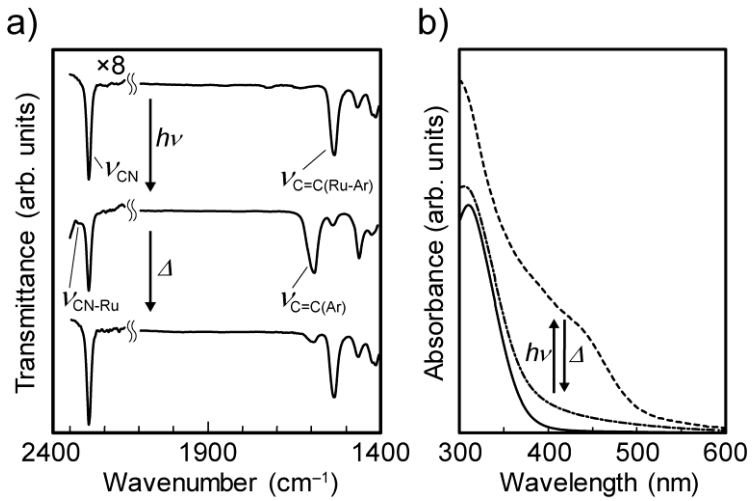

Fig. S5. (a) FT-IR and (b) UV–Vis spectra of IL **1b**, CP **2b**, and after heating **2b** at 90 °C for 2 h.

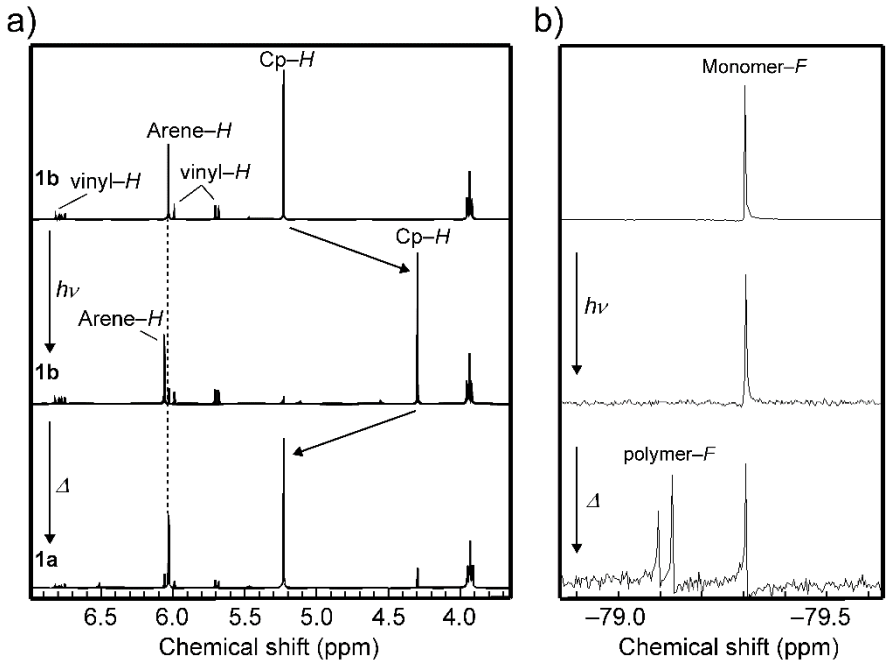

Fig. S6. (a) ^{1}H NMR and (b) ^{19}F NMR spectra (400 MHz, CD_3CN) of IL **1b**, CP **2b**, and after heating **2b** at 120 °C for 12 h.

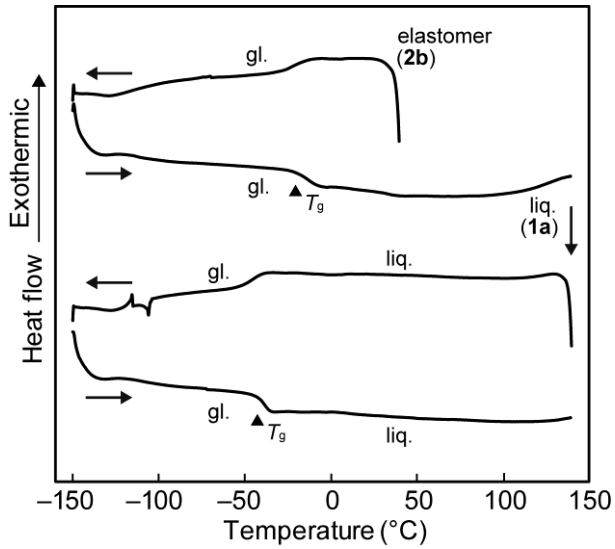

Fig. S7. DSC traces of CP **2b** (10 °C min^{-1}) where liq. and gl. are the liquid and glassy states, respectively.

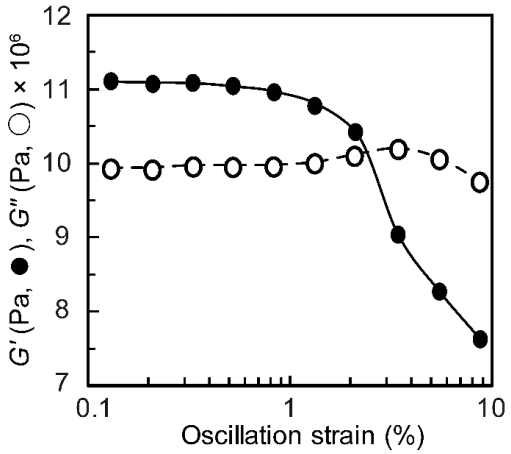

Fig. S8. Oscillation strain dependence of the storage modulus (●) and loss modulus (○) of IL **1b** (angular frequency: 400 rad s^{-1}).

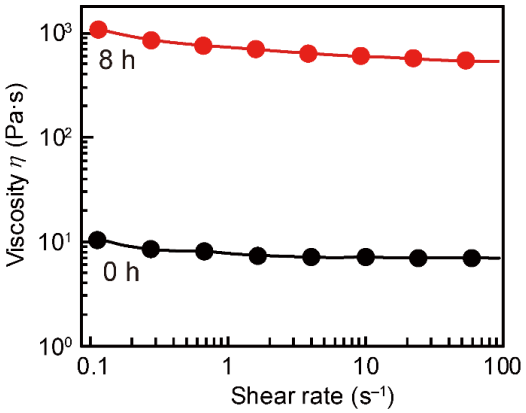

Fig. S9. Shear rate dependence of viscosities for IL **1b** and CP **2b** (after 8 h photoirradiation).

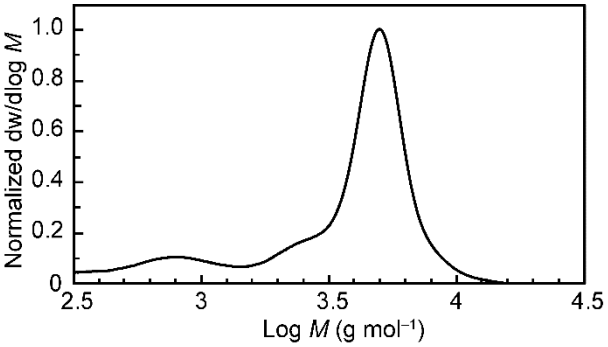

Fig. S10. Molecular weight distribution curve of PIL **1a** relative to polystyrene standards as determined by GPC/SEC (eluent: DMF containing 10 mM LiBr).